Journal of Mines, Metals and Fuels, *73(1): 199-209; 2025. DOI: 10.18311/jmmf/2025/47458*

Print ISSN : 0022-2755

Journal of Mines, Metals and Fuels

Contents available at: *www.informaticsjournals.co.in/index.php/jmmf*

Study of Influence of Hole Distance on the Strength of Locking Compression Plate Implants

Ishan R. Sathone* and Umesh G. Potdar

Department of Mechanical Engineering, Pimpri Chinchwad College of Engineering, Pune - 411044, Maharashtra, India; ishan.7315@gmail.com

Abstract

Locking Compression Plate (LCP) implants have become an increasingly popular choice for orthopaedic surgeries, particularly in treating tibia bone fractures. Tibia implants have a failure rate from 7% to 18%. This study aimed to investigate the influence of the distance between the holes in the LCP implants on their overall strength and mechanical stability. The researchers employed a finite element analysis approach to simulate the performance of LCP implants made of Ti6Al4V Titanium Alloy. As Ti6A14V Titanium alloy has superior corrosion resistance, biocompatibility, and lower modulus of elasticity, which distribute stress evenly, we have selected this material for our study. This comparative analysis suggests that increasing the distance between the holes from 5mm to 8mm in the LCP implant can enhance mechanical stability and load-bearing capacity. Finite element analysis suggested that the increase in hole distance from 5mm to 8mm reduced the stress value from 89.541 MPa to 81.734 MPa. The stresses in the implant increased to 88.025 MPa after increasing the hole distance beyond 8mm. These insights can inform the optimization of LCP implant design, particularly in treating tibia bone fractures, to ensure secure fixation and improved patient clinical outcomes.

Major Findings: *Increasing the hole distance in the LCP implant from 5 mm to 8 mm enhances mechanical stability and reduces stress from 89.541 MPa to 81.734 MPa. However, increasing the distance beyond 8 mm raises the stress to 88.025 MPa, making the implant unstable. The inverse correlation exists between the hole distance and maximum stress magnitude.*

Keywords: *Finite Element Analysis, Implant Strength, Locking Compression Plate, Tibia Bone, Ti6Al4V Alloy*

1.0 Introduction

The tibia is the larger and stronger of the two bones in the lower leg, situated medially to the fibula. It connects to the femur (thigh bone) at the knee joint and to the talus (ankle bone) at the ankle joint. The tibia has a relatively straight shaft with a slightly expanded proximal end that forms part of the knee joint and a distally expanded end that forms part of the ankle joint[1]. Numerous muscles involved in leg movement attach to the tibia. These include the quadriceps (for knee extension), hamstrings (for knee flexion), and calf muscles (for ankle movement). The Tibia bone is biomechanically stable and specialized to bear the compressive force of the body weight. The bone frame is a straight beam with an extended head at the proximal portion. When excessive force is applied to the bones, the crack is initiated, causing the bone to shatter or break. This is termed a "Bone Fracture"[2,3]. The implants were introduced in the 19th century, but the use of implants in vivo was very rare. The involvement of engineers in designing the implants was very limited. The orthopaedic surgeons were called innovators of implants in that era[4]. Bone fracture treatment generally involves one of three main approaches. Simpler fractures can often be treated with casting, where a hard bandage immobilizes the bone to allow natural healing. More complex fractures may

**Author for correspondence*

require open reduction and internal fixation, a surgical procedure where the bone is realigned and stabilized using internal metal implants. For severe fractures or those unsuitable for ORIF, open reduction and external fixation are used. This method involves surgically aligning the bone and then stabilizing it with an external frame that supports healing. The choice of treatment depends on the complexity and severity of the fracture[5–7].

Various studies have indicated that after a patient undergoes the procedure and operations for fracture, the implants may fail, and the failure rate of the implant may vary from 7% to 18%[8–10]. After the failure, patients must again undergo retreatment, and this causes a financial and mental burden on the patient. The causes for failure of the implant can be divided into three major categories:

Failures are due to patient-specific factors, such as age, weight, physical activity level, diabetes, smoking, etc. Surgical techniques include improper selection and placement of implants, among others. Implant factors include improper implant manufacturing, implant design, the biocompatibility of material selected for the implant, etc.

The implants are designed considering the average body mass index; hence, the failure rate of tibia implants is up to 7.3%[11]. Different testing standards are available for implants like ASTM F3140, ASTM F1800, etc.[12,13]. Modifications in design can greatly reduce the tibia implant failure rate to a great extent[14,15].

Orthopaedic implants have become increasingly common in treating bone injuries and conditions. Two popular materials used in these implants are stainless steel (SS 316L) and titanium alloy (Ti6Al4V)[16,17]. Locking Compression Plate (LCP) implants have become an increasingly preferred choice for treating tibia bone fractures due to their superior biomechanical properties and improved fixation stability. The design of these implants, including the selection of materials and the spacing between the holes, can significantly impact their mechanical strength and long-term performance[2,18–20]

Biomechanical studies have highlighted the importance of implant design in ensuring secure fixation and load transfer to the surrounding bone[21]. Factors such as material properties, surface geometry, and screw placement can all contribute to the overall performance of LCP implants[7,22–27]. Recent advancements in additive manufacturing techniques have also enabled the development of patient-specific implants, further emphasizing the need to optimize the design parameters for improved clinical outcomes. The ability to customize implant designs to match individual patient anatomy and loading conditions can lead to enhanced load distribution, better stress transfer to the bone, and, ultimately, improved long-term outcomes for patients.

The choice of material is crucial, as it can significantly impact the biomechanical performance and long-term success of the implant. Stainless steel, such as SS 316L, has been widely used in orthopaedic implants due to its strength and corrosion resistance. However, the relatively high elastic modulus of stainless steel can lead to stress shielding, a phenomenon where the implant bears a disproportionate amount of the load, resulting in the reabsorption of natural bone and implant loosening. In contrast, titanium alloys, like Ti6Al4V, have a lower elastic modulus that more closely matches the properties of human bone[28–30]. This helps to mitigate the issue of stress shielding and promotes better integration between the implant and the surrounding bone tissue. In addition to the material selection, the design of the implant, including the distance between the holes in an LCP implant, can also significantly impact the overall strength and performance of the implant-bone assembly.

To better understand the influence of the hole distance on the strength of LCP implants, we conducted a comparative study on the performance of SS 316L steel and Ti6Al4V alloy implants when applied to the tibia bone. In this context, the present study aimed to evaluate the impact of hole distance on the strength of LCP implants made from SS 316L Steel and Ti6Al4V Alloy. In the present study, we investigate the impact of the distance between the holes in Locking Compression Plate implants made of Ti6Al4V alloy on the overall strength and performance of the implant when applied to the tibia bone. By analysing factors such as stress distribution and overall mechanical stability through finite element analysis, this research could provide valuable insights to guide the optimization of LCP implant design and ultimately enhance clinical outcomes in treating tibia bone fractures.

The findings of this research could provide valuable insights for orthopaedic surgeons and implant manufacturers in selecting the most suitable LCP design for tibia bone fracture treatment.

2.0 Materials and Methods

A finite element analysis approach was employed to simulate the performance of LCP implants made of Ti6Al4V Alloy. The Ti6Al4V alloy LCP implant exhibited superior biomechanical properties compared to the SS 316L steel implant. The titanium alloy's lower elastic modulus helped mitigate the issue of stress shielding, a common problem associated with hard tissue implants. The external shape of the implant was designed based on the geometric data obtained from the catalogues of various implant manufacturers[31]. The implants were modelled with varying distances between the holes, and their mechanical behaviour was analysed under simulated loading conditions. The width of the plate and thickness of the plate are kept constant as shown in Figure 1, whereas the centre distance of holes was varied from 5 mm to 10mm.

The bone model is developed considering the average length of the tibia bone, the lateral, anterior, and medial cross sections[1] as shown in Figure 2. The Young's modulus and poisons ratio for the bone is considered to

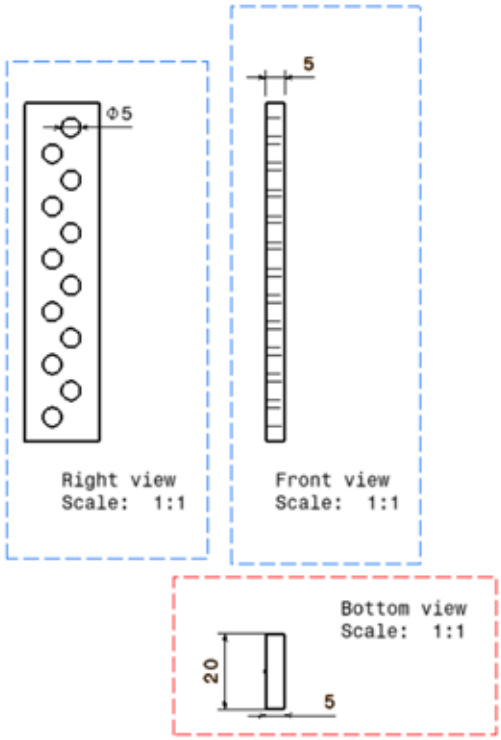


Figure 1. Implant plate dimensions (all dimensions are in mm)

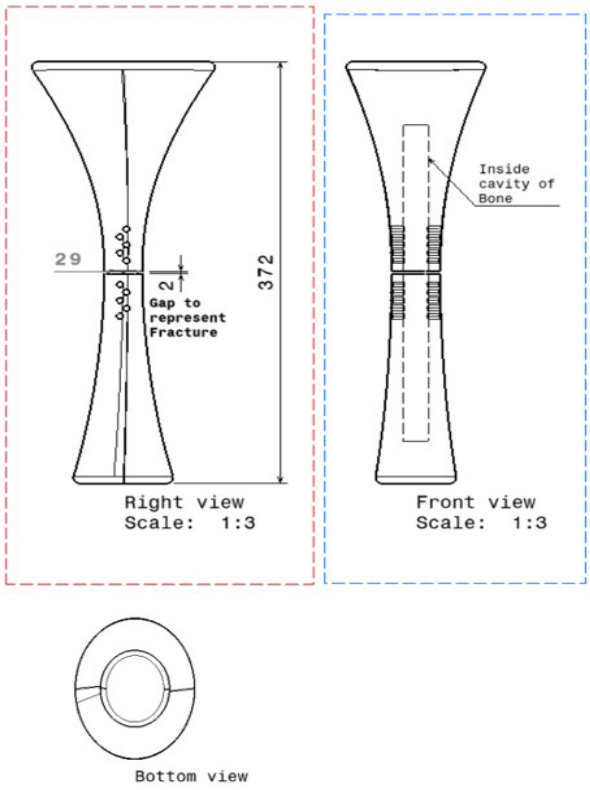


Figure 2. Tibia bone dimensions (all dimensions are in mm)

be 14 GPa and 0.488[33,34]. The superior biocompatibility and corrosion resistance of Ti6Al4V alloy facilitated better integration between the implant and the surrounding bone tissue, which is crucial for long-term implant stability and performance. Figure 3 shows the boundary conditions used for the simulation. One end of the bone is fixed, ensuring that all degrees of freedom of the end surface is zero, and on the other end, a force of 1101.7 N is applied. The load of 1101.7 N is identified from the literature as it is the load acting during walking at a self-selected speed[2]. During the simulation, it was observed that the fracture gap was filling, and the upper and lower bones were meeting each other. Considering this, the frictional contact between the upper and lower bone is applied in Figure 4. The contact between the implant screw, bone, and implant plate is taken as bonded contact to avoid any separation from the respective surfaces. The Young's modulus and poisons ratio for the Ti6Al4V alloy are considered 96 GPa and 0.36[35], respectively, and incorporated into the finite element models. The bone-implant interface was assumed to be

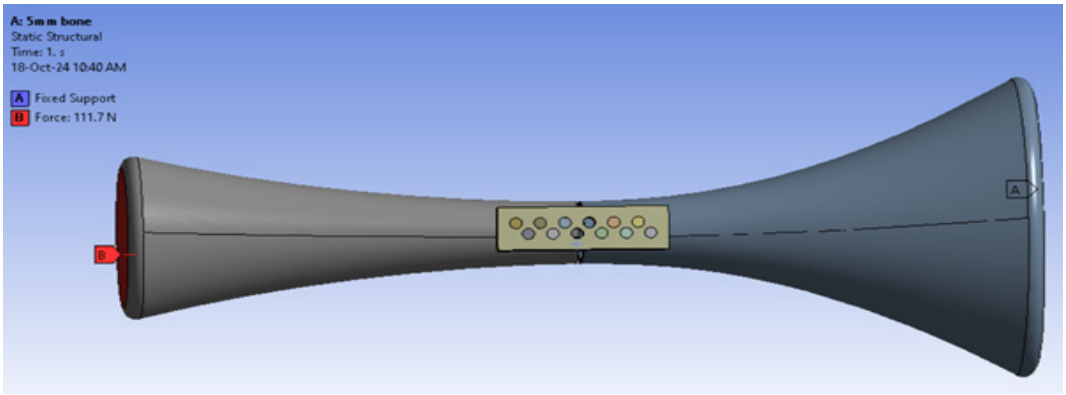


Figure 3. Boundary conditions.

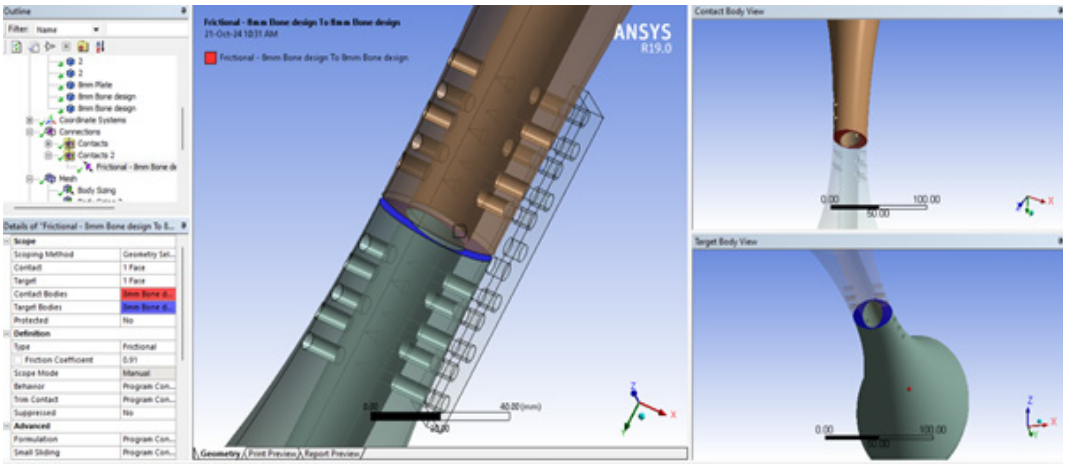


Figure 4. Contact considerations for fracture gap.

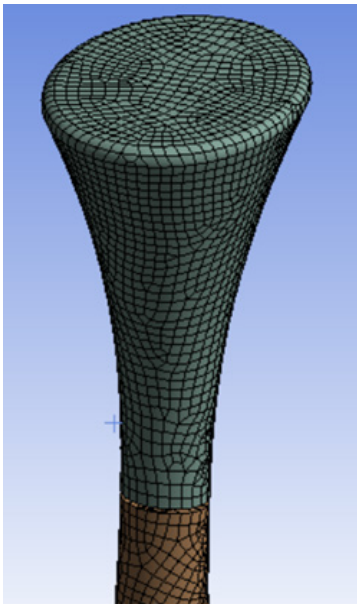


Figure 5. Representation of meshing for tibia bone (5mm hexahedron elements).

perfectly bonded, and the boundary conditions were applied to simulate the loading scenarios encountered during normal physiological activities. We simulated the LCP implant for the tibia bone using Ti6Al4V alloy as the implant material. The simulations were conducted using a commercial finite element software package (Ansys R19.0), and the results were analysed to assess the impact of hole distance on the stress distribution, strain, and overall mechanical stability of the LCP implants.

Figure 5 to Figure 7 shows the meshing and type of elements used for the simulation. Considering the body size and geometry, we have used the hexahedron elements for bone and implant plates with 5 mm and 2 mm element sizes, respectively. To accommodate the geometry feature of the implant screw, the tetrahedron elements with an element size of 1 mm are considered.

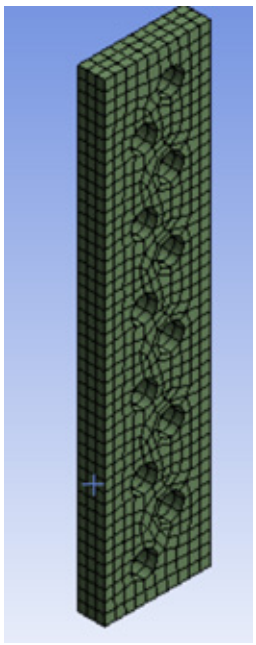


Figure 6. Representation of meshing for implant plate (2mm hexahedron elements).

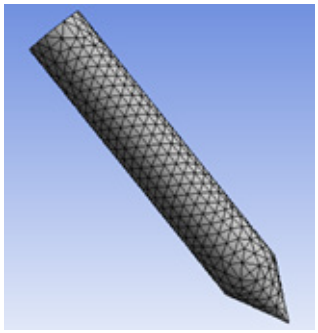


Figure 7. Representation of meshing for implant screw (1mm tetrahedron element).

3.0 Results and Discussion

Figures 8 to 19 show the stress distribution on implant and bone obtained from the simulation. Tables 1 to 6 show the value of maximum stress distribution for different hole distances on the LCP. The finite element analysis revealed that the distance between holes had a significant impact on the mechanical performance of the LCP implants. As the distance between holes increased, the overall strength and stability of the implants improved, with a more even distribution of stresses and reduced risk of localized failure. This can be attributed to the superior mechanical properties of Ti6Al4V Alloy, such as its higher tensile strength and fracture toughness.

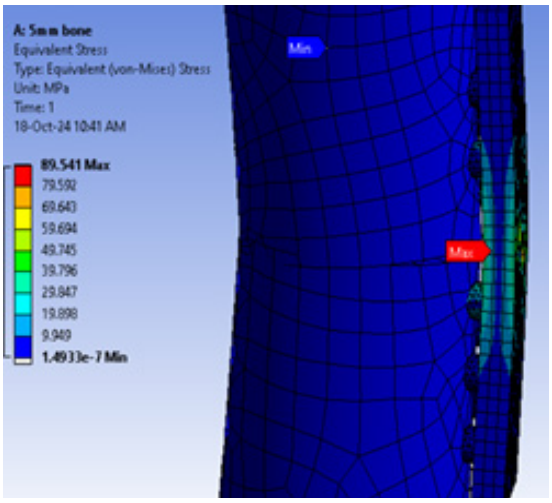


Figure 8. Assembly view of stresses generated in 5mm hole distance implant plate, bone and screw.

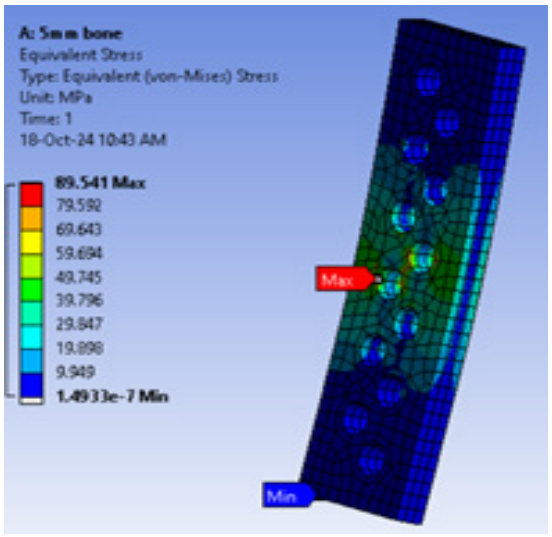


Figure 9. Component view of stress generated in 5mm hole distance implant plate.

Table 1. Maximum stress value for 5mm hole distance

Time (Sec)	Maximum Stress Values (MPa)
0.2	17.918
0.4	35.834
0.7	62.696
1.	89.541

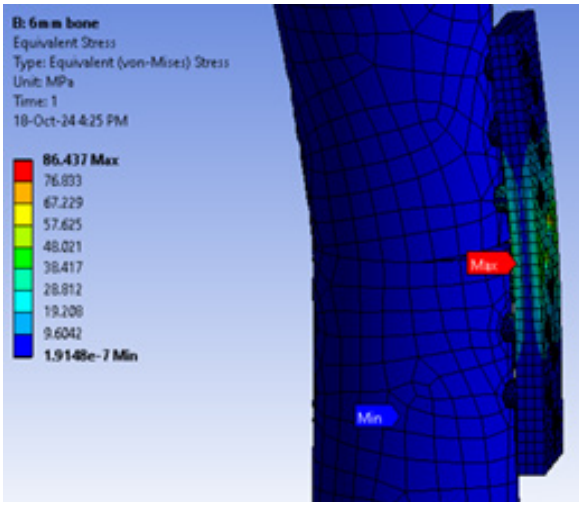


Figure 10. Assembly view of stresses generated in 6mm hole distance implant plate, bone and screw.

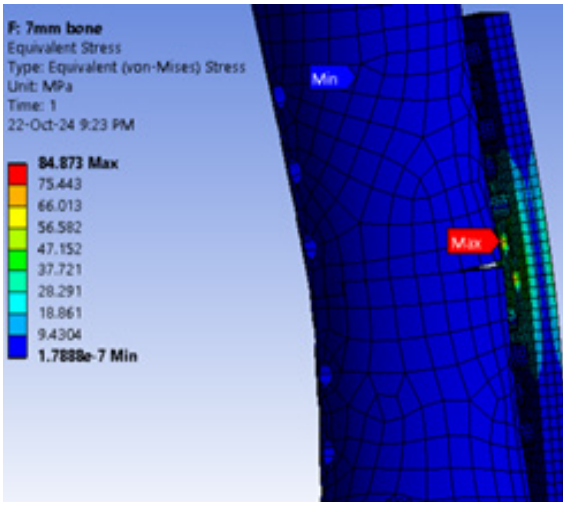


Figure 12. Assembly view of stresses generated in 7mm hole distance implant plate, bone and screw.

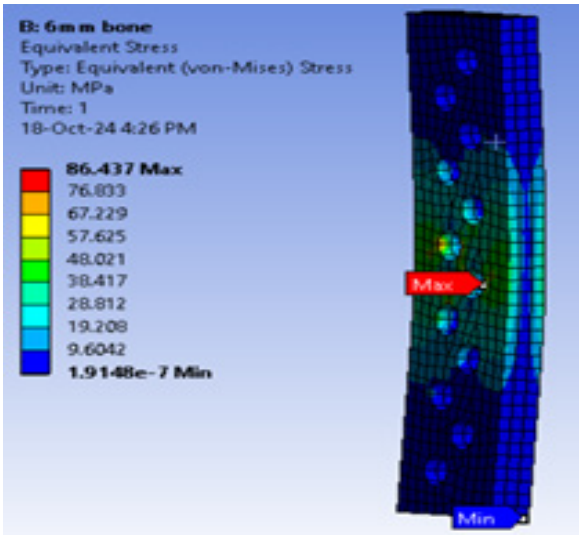


Figure 11. AComponent view of stresses generated in 6mm hole distance implant plate..

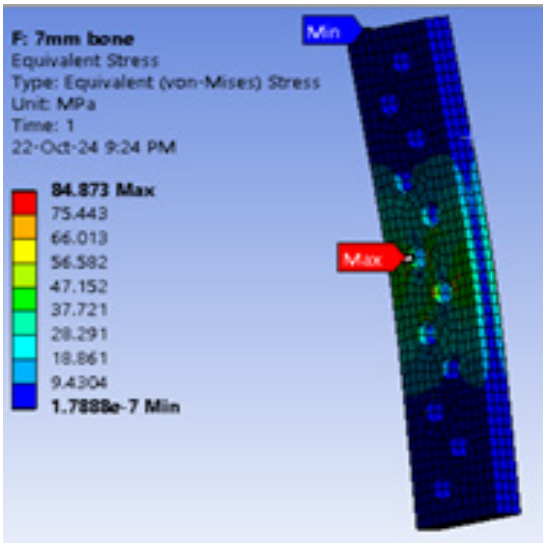


Figure 13. Component view of stresses generated in 7mm hole distance implant plate.

Table 2. Maximum stress value for 6mm hole distance

Time (Sec)	Maximum Stress Values (MPa)
0.2	17.295
0.4	34.59
0.7	60.52
1.	86.437

Table 3. Maximum stress value for 7mm hole distance

Time (Sec)	Maximum Stress Values (MPa)
0.2	16.98
0.4	33.961
0.7	59.422
1.	84.873

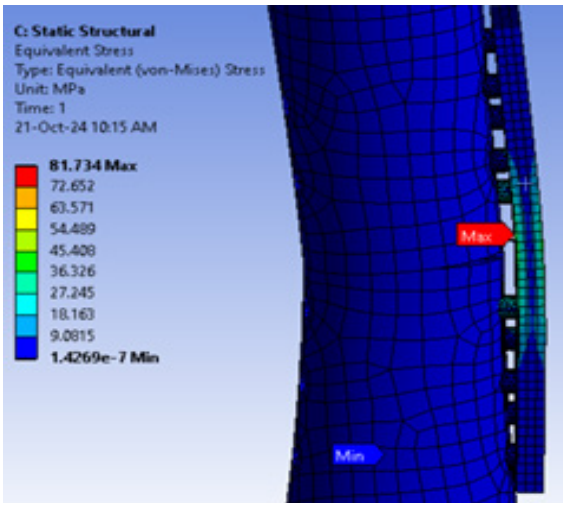


Figure 14. Assembly view of stresses generated in 8mm hole distance implant plate, bone and screw.

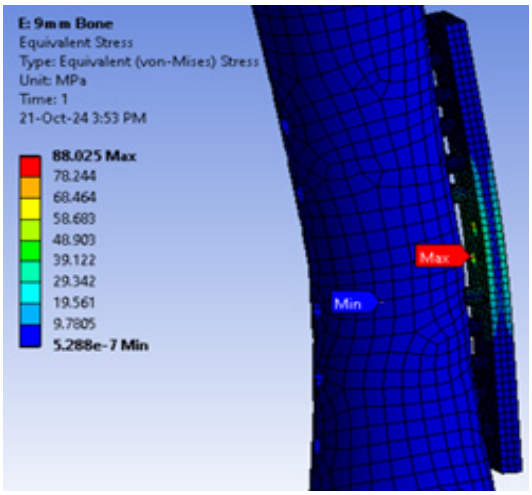


Figure 16. Assembly view of stresses generated in 9mm hole distance implant plate, bone and screw.

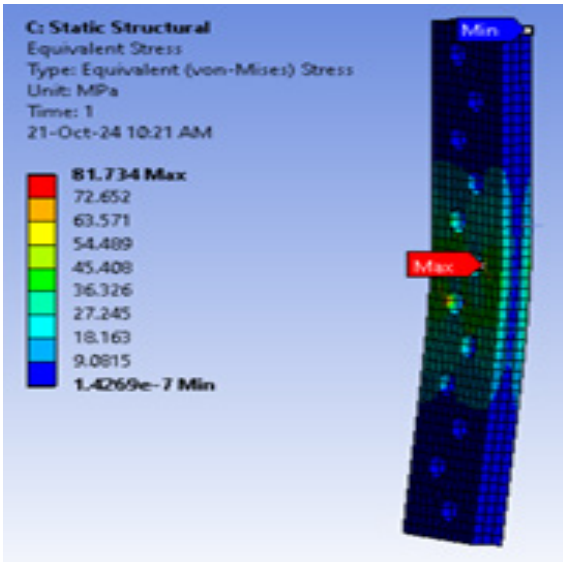


Figure 15. Component view of stresses generated in 8mm hole distance implant plate.

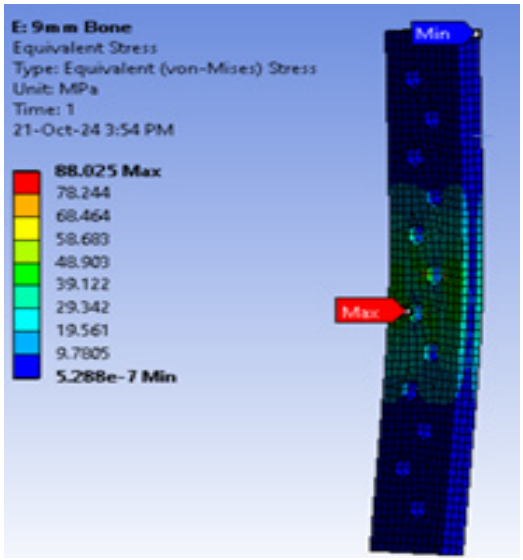


Figure 17. Component view of stresses generated in 9mm hole distance implant plate.

Table 4. Maximum stress value for 8 mm hole distance

Time (Sec)	Maximum Stress Values (MPa)
0.2	16.351
0.4	32.702
0.7	57.222
1.	81.734

Table 5. Maximum stress value for 9 mm hole distance

Time (Sec)	Maximum Stress Values (MPa)
0.2	17.609
0.4	35.217
0.7	61.624
1.	88.025

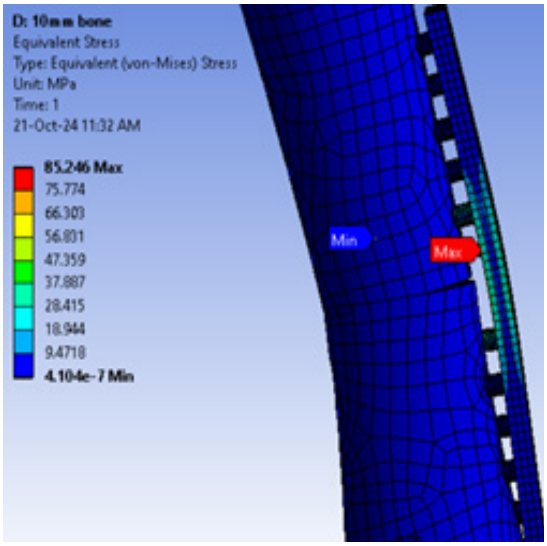


Figure 18. Assembly view of stresses generated in 10mm hole distance implant plate, bone and screw.

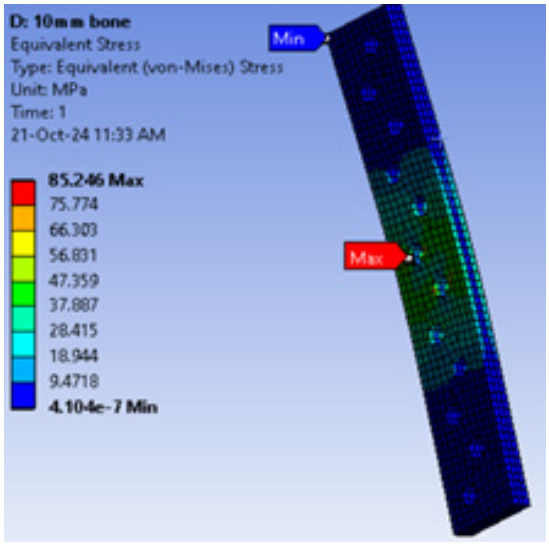


Figure 19. Component view of stresses generated in 10mm hole distance implant plate.

Table 6. Maximum stress value for 10 mm hole distance

Time (Sec)	Maximum Stress Values (MPa)
0.2	17.052
0.4	34.103
0.7	59.677
1.	85.246

Table 7 shows the values of maximum Von Mises stress for varying hole distances, and the same values are used to create the plot shown in Figure 20. From the graph, it is very evident that the increase in the hole distance from 5mm to 8 mm gradually decreases the stress value from 89.541 MPa to 81.734 MPa in the implant plate. Also, the increase in distance between the holes beyond 8 mm will increase the stress value significantly to 88.025 MPa, making the implant less stable and may cause its failure. As the distance between the holes increases, the load applied on the implant plate is distributed to a larger area reducing the stresses in the implant. These results suggest that careful consideration of the distance between holes in LCP implant design and the selection of appropriate

Table 7. Compilation of results generated for maximum stress by varying hoke distance

Sr. No.	Distance between the holes (mm)	Maximum Stress generated during simulation (MPa)
1	5	89.541
2	6	86.437
3	7	84.873
4	8	81.734
5	9	88.025
6	10	85.246

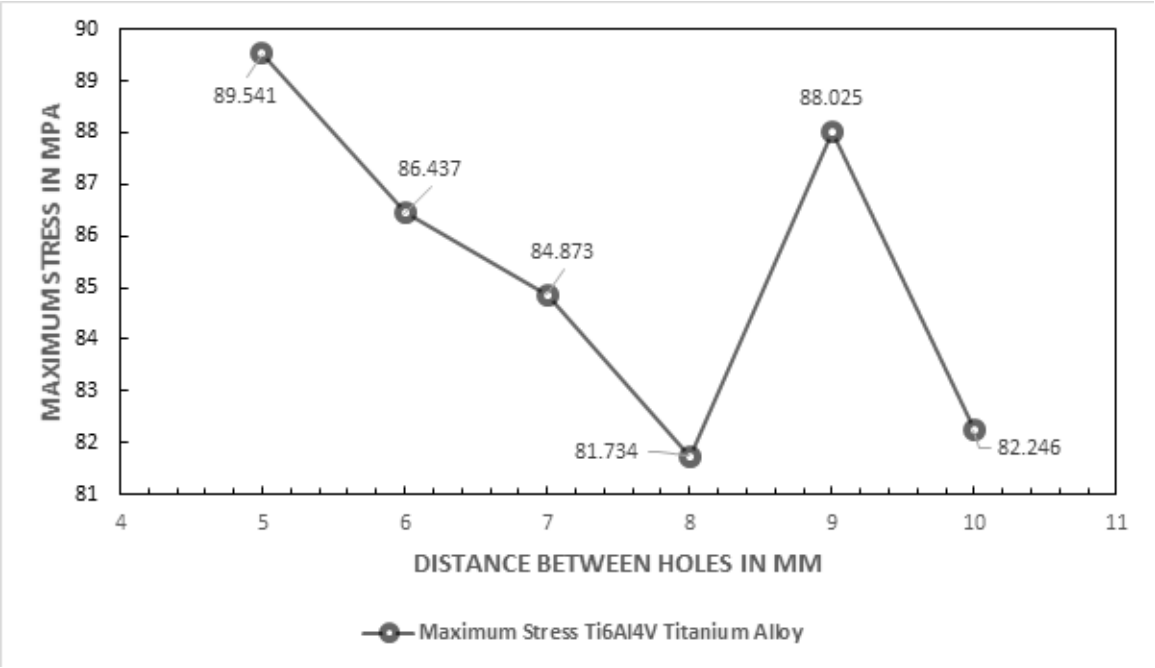


Figure 20. Representation of hole distance vs maximum stress.

material can contribute to the overall success of tibia bone fracture treatment.

4.0 Conclusion

Implant design, including the distance between the holes in locking compression plate implants, plays a crucial role in the overall strength and performance of the implant-bone assembly. As it is evident from the results increasing the distance between the holes from 5mm to 8mm was reducing the stresses from 89.541 MPa to 81.734 MPa. Further increasing the hole distance to 9mm made the implant plate unstable as the stresses increased to 88.025 MPa. The superior biomechanical performance of the Ti6Al4V alloy LCP implant and the benefits of optimizing the distance between the holes can contribute to improved patient outcomes and reduced risk of implant failure. The comparative analysis suggests that increasing the distance between the holes from 5mm to 8mm in the LCP implant can enhance mechanical stability and load-bearing capacity. The results of this study highlight the importance of considering the material properties and the geometric parameters of the implants to optimize their performance and long-term success. The findings can guide orthopaedic surgeons and implant manufacturers in selecting the most appropriate LCP implant design for tibia bone fracture treatment, ultimately leading to improved patient outcomes. With the advancement of new technologies like 3D printing, we can design patient-specific implants, which will further reduce the failure rate of the implant.

5.0 References

1. Quintens L, Herteleer M, Vancleef S, Carette Y, Duflou J, Nijs S, et al. Anatomical variation of the tibia—a principal component analysis. Sci Rep. 2019; 9(1):1–10. https://doi.org/10.1038/s41598-019-44092-8. PMID: 31114000; PMCID: PMC6529455.
2. D'Angeli V, Belvedere C, Ortolani M, Giannini S, Leardini A. Load along the tibial shaft during activities of daily living. J Biomech. 2014; 47(5):1198–205. https://doi.org/10.1016/j.jbiomech.2014.01.045. PMID: 24548336.
3. Thompson GH, Wallace A, Son-hing JP. Fractures of the tibia and fibula. In: Green's skeletal trauma in children. 5th ed. Elsevier; 2014. p. 437–72. https://doi.org/10.1016/B978-0-323-18773-2.00016-0. PMCID: PMC4387038.
4. Markatos K, Tsoucalas G, Sgantzos M. Hallmarks in the history of orthopaedic implants for trauma and joint replacement. Acta Med Hist Adriat. 2016. Available from: https://pubmed.ncbi.nlm.nih.gov/27598960/

5. Lichte P, Pape HC. Tibial shaft fractures. Bone Jt Inj Trauma Surg III. 2014; 46(2):341–6. https://doi.org/10.1016/S2255-4971(15)30227-5
6. Schmidt AH, Finkemeier CG, Tornetta P. Treatment of closed tibial fractures. Instr Course Lect. 2003; 52:607–22. https://doi.org/10.2106/00004623-200302000-00027. PMID: 12690886.
7. Egol KA, Kubiak EN, Fulkerson E, Kummer FJ, Koval KJ. Biomechanics of locked plates and screws. J Orthop Trauma. 2004; 18(8):488–93. https://doi.org/10.1097/00005131-200409000-00003. PMID: 15475843.
8. Ruiz AL, Kealey WDC, McCoy GF. Implant failure in tibial nailing. Injury. 2000; 31(5):359–62. https://doi.org/10.1016/S0020-1383(00)00002-4. PMID: 10775692.
9. Keohane D, Sheridan GA, Masterson E. High rate of tibial debonding and failure in a popular knee replacement. Bone Jt Open. 2022; 3(6):495–501. https://doi.org/10.1302/2633-1462.36.BJO-2022-0043.R1. PMID: 35698801; PMCID: PMC9233423.
10. Jemt T, Olsson M, Franke Stenport V. Incidence of first implant failure: A retrospective study of 27 years of implant operations at one specialist clinic. Clin Implant Dent Relat Res. 2015; 17(S2):e501–10. https://doi.org/10.1111/cid.12277
11. Ruiz AL, Kealey WDC, McCoy GF. Implant failure in tibial nailing. Injury. 2000; 31(5):359–62. https://doi.org/10.1016/S0020-1383(00)00002-4. PMID: 10775692.
12. Clary C, Maletsky L. Mechanical testing of knee implants. In: Mechanical testing of orthopaedic implants. Elsevier Ltd; 2017. p. 207–29. https://doi.org/10.1016/B978-0-08-100286-5.00011-1
13. Friis EA, Tsao AK, Timmie Topoleski LD, Jones LC. Introduction to mechanical testing of orthopaedic implants. In: Mechanical testing of orthopaedic implants. Elsevier Ltd; 2017. p. 3–15. https://doi.org/10.1016/B978-0-08-100286-5.00001-9. PMID: 28096898; PMCID: PMC5234258.
14. De Onis M. WHO child growth standards based on length/height, weight and age. Acta Paediatr Int J Paediatr. 2006; 450:76–85. https://doi.org/10.1111/j.1651-2227.2006.tb02378.x. PMID: 16817681.
15. Friis EA, Abel D, Woods T. Influence of standards organizations and regulatory agencies in the mechanical testing of orthopaedic implants. In: Mechanical testing of orthopaedic implants. Elsevier Ltd; 2017. p. 49–60. https://doi.org/10.1016/B978-0-08-100286-5.00004-4
16. Manivasagam G, Dhinasekaran D, Rajamanickam A. Biomedical implants: corrosion and its prevention—a review. Recent Patents Corros Sci. 2010; 2(1):40–54. https://doi.org/10.2174/1877610801002010040
17. Navarro M, Michiardi A, Castaño O, Planell JA. Biomaterials in orthopaedics. J R Soc Interface. 2008; 5(27):1137–58. https://doi.org/10.1098/rsif.2008.0151. PMID: 18667387; PMCID: PMC2706047.
18. Isaksson H. Recent advances in mechanobiological modelling of bone regeneration. Mech Res Commun. 2012; 42:22–31. https://doi.org/10.1016/j.mechrescom.2011.11.006
19. Giacaglia GEO, Lamas W de Q. Pedicle screw rupture: a case study. Case Stud Eng Fail Anal. 2015; 4:64–75. https://doi.org/10.1016/j.csefa.2015.09.001
20. Bel JC. Pitfalls and limits of locking plates. Orthop Traumatol Surg Res. 2019; 105(1): S103–9. https://doi.org/10.1016/j.otsr.2018.04.031. PMID: 30130659.
21. Stoffel K, Dieter U, Stachowiak G, Gächter A, Kuster MS. Biomechanical testing of the LCP: how can stability in locked internal fixators be controlled? Injury. 2003; 34(SUPPL. 2). https://doi.org/10.1016/j.injury.2003.09.021. PMID: 14580982.
22. Rice D, Shaat M. Reporting the fatigue life of 316L stainless steel locking compression plate implants: the role of the femoral and tibial biomechanics during the gait. J Biomech Eng. 2017; 139(10). https://doi.org/10.1115/1.4037561. PMID: 28787474.
23. Lenz M, Windolf M, Mückley T, Hofmann GO, Wagner M, Richards RG, et al. The locking attachment plate for proximal fixation of periprosthetic femur fractures—a biomechanical comparison of two techniques. Int Orthop. 2012; 36(9):1915–21. https://doi.org/10.1007/s00264-012-1574-x. PMID: 22638607; PMCID: PMC3427437.
24. Ahmad M, Nanda R, Bajwa AS, Candal-Couto J, Green S, Hui AC. Biomechanical testing of the locking compression plate: when does the distance between bone and implant significantly reduce construct stability? Injury. 2007; 38(3):358–64. https://doi.org/10.1016/j.injury.2006.08.058. PMID: 17296199.
25. Miller DL, Goswami T. A review of locking compression plate biomechanics and their advantages as internal fixators in fracture healing. Clin Biomech (Bristol, Avon). 2007; 22(10):1049–62. https://doi.org/10.1016/j.clinbiomech.2007.08.004. PMID: 17904257.
26. Eichinger JK, Herzog JP, Arrington ED. Analysis of the mechanical properties of locking plates with and without screw hole inserts. Orthopedics. 2011; 34(1). https://doi.org/10.3928/01477447-20101123-13. PMID: 21210620.

27. Sommer C, Babst R, Müller M, Hanson B. Locking compression plate loosening and plate breakage: a report of four cases. J Orthop Trauma. 2004; 18(8):571–7. https://doi.org/10.1097/00005131-200409000-00016. PMID: 15475856.
28. Chen Q, Thouas GA. Metallic implant biomaterials. Mater Sci Eng R Rep. 2015; 87:1–57. https://doi.org/10.1016/j.mser.2014.10.001
29. Niinomi M, Nakai M. Titanium-based biomaterials for preventing stress shielding between implant devices and bone. Int J Biomater [Internet]. 2011. https://doi.org/10.1155/2011/836587 PMID:21765831 PMCID: PMC3132537
30. Niinomi M, Liu Y, Nakai M, Liu H, Li H. Biomedical titanium alloys with Young's moduli close to that of cortical bone. Regen Biomater [Internet]. 2016; 3(3):173–85. https://doi.org/10.1093/rb/rbw016 PMID:27252887 PMCID: PMC4881615
31. DePuy Synthes. LCP locking compression plate surgical technique [Internet]. 2004. Available from: http://synthes.vo.llnwd.net/o16/LLNWMB8/INT%20Mobile/Synthes%20International/Product%20Support%20Material/legacy_Synthes_PDF/164842.pdf
32. Attada P, Ravindranadh G, Kumari K. Anthropometric measurement of maximum tibia length in South Indian population. Anat Sci [Internet]. 2018; 15(2):57–64. Available from: www.graphpad.com/quickcalcs/linear2/
33. Rho JY, Ashman RB, Turner CH. Young's modulus of trabecular and cortical bone material: ultrasonic and micro tensile measurements. J Biomech [Internet]. 1993; 26(2):111–9. https://doi.org/10.1016/0021-9290(93)90042-D PMID:8429054
34. Arjmand H, Nazemi M, Kontulainen SA, McLennan CE, Hunter DJ, Wilson DR, et al. Mechanical metrics of the proximal tibia are precise and differentiate osteoarthritic and normal knees: A finite element study. Sci Rep. 2018; 8(1):1–10. https://doi.org/10.1038/s41598-018-29880-y PMID:30065276 PMCID: PMC6068127
35. Zhao J, Wang Z, Tian L, Wan J, Zong X, Zhang S, *et al.* Study on mechanical properties of Ti-6Al-4V titanium alloy with different microstructures under combined tension-bending load. J Alloys Compd. 2023; 936:168201. https://doi.org/10.1016/j.jallcom.2022.168201